Separation Science and Technology
Publication details, including instructions for authors and subscription information:
http://www.informaworld.com/smpp/title~content=t713708471

Pervaporation of Ethanol and Acetone above Normal Boiling Temperatures

Dario Windmöller[a]; Fernando Galembeck[b]
[a] Institute de Ciĕncias, Tecnologia e Saúde, Universidade de Ijuí, Ijuí, RS, Brasil [b] INSTITUTE OF CHEMISTRY UNIVERSIDADE ESTADUAL DE CAMPINAS, CAMPINAS, SP, BRAZIL

To cite this Article Windmöller, Dario and Galembeck, Fernando(1992) 'Pervaporation of Ethanol and Acetone above Normal Boiling Temperatures', Separation Science and Technology, 27: 10, 1183 — 1196
To link to this Article: DOI: 10.1080/01496399208019419
URL: http://dx.doi.org/10.1080/01496399208019419

SEPARATION SCIENCE AND TECHNOLOGY, 27(10), pp. 1183–1196, 1992

Pervaporation of Ethanol and Acetone above Normal Boiling Temperatures

DARIO WINDMÖLLER* and FERNANDO GALEMBECK
INSTITUTE OF CHEMISTRY
UNIVERSIDADE ESTADUAL DE CAMPINAS
CAIXA POSTAL 6154, 13081 CAMPINAS, SP, BRAZIL

Abstract

Pervaporation experiments were performed at higher than normal feed liquid boiling temperatures by applying pressure to the feed compartment. Ethanol, acetone, and aqueous ethanol solutions were pervaporated through silicone rubber dense membranes. Large increases were observed in the permeate flow as the temperature rose above the liquid boiling temperature. Separation factors in aqueous ethanol pervaporation are not affected by these increases in permeate output, and they are in the same range as those obtained in conventional pervaporation.

INTRODUCTION

In the last few years, pervaporation has developed to become a unit operation used in full-sized plants in ethanol dehydration (*1*).

The introduction of new, more effective membranes will probably increase the efficiency and broaden the applicability of pervaporation as experience and reliability in its use build up.

Another approach to improve pervaporation scope and efficiency, as in any other membrane separation process, is the optimization of operation parameters and fluid management.

The effects of temperature, feed pressure, and effluent pressure can be estimated within current pervaporation models (*2*, *3*). The temperature effect on permeate flow can be predicted by using the relevant activation energy. Feed pressure is predicted to have modest effects, unless the pressure is sufficiently high to approach the levels required for reverse osmosis.

*Permanent address: Instituto de Ciências, Tecnologia e Saúde, Universidade de Ijuí, 98700 Ijuí, RS, Brasil.

Effluent pressure is an interesting and more complex variable, and its effect can be shown by taking the data of different authors on water–ethanol pervaporation through regenerated cellulose membranes. In vacuum pervaporation experiments, water permeates cellulose faster than ethanol; on the other hand, in sweeping gas pervaporation, ethanol permeates faster than water. This difference can be easily understood: in vacuum, the surface of the membrane is strongly dehydrated, and since the affinity of cellulose is greater for water than for ethanol, the former will migrate preferentially through the membrane. In sweeping gas pervaporation, the membrane is soaked with aqueous ethanol solution on both sides. What the sweeping gas contacts is a three-component (cellulose, water, ethanol) gel, from which the more volatile component desorbs faster than the less volatile water.

In recent work we have shown that it should be possible to do isothermal pervaporation experiments by using feed pressures of a few tens of atmospheres (*4*, *5*). These experiments are attractive because they are equivalent to isothermal distillation and thus should have low energy consumption.

During these experiments we observed that the pervaporation rate increases many-fold as we increase the temperature above normal boiling temperature of the feed liquid. This is a new experimental result which has not been predicted for current pervaporation models (*2*, *3*).

This is a report on the pervaporation of ethanol, acetone, and aqueous ethanol solutions using feed pressures in the 0.3–1.4 MPa range, temperatures above as well as below normal boiling temperatures, and room pressure in the effluent compartment under the stagnant atmosphere.

EXPERIMENTAL

The pervaporation cell was built of carbon steel with a corrosion-resistant coating by Staubli (Diadema, São Paulo); it was tested to stand 5 MPa pressure. An exploded schematic view of the cell is given as Fig. 1. The cell was connected to a feed solution reservoir kept under pressure from a nitrogen cylinder. The cell was heated with a heating strap connected to an autotransformer. The internal cell temperature was measured by using a thermocouple mounted on the membrane holding plate. The external cell temperature was also measured.

The membranes were cast by spreading toluene solutions of Dow-Corning 732 RTV Silastic adhesive over PVC-coated glass sheets, as in previous work from this laboratory (*4*, *5*). Nichrome wires were used to limit membrane thickness.

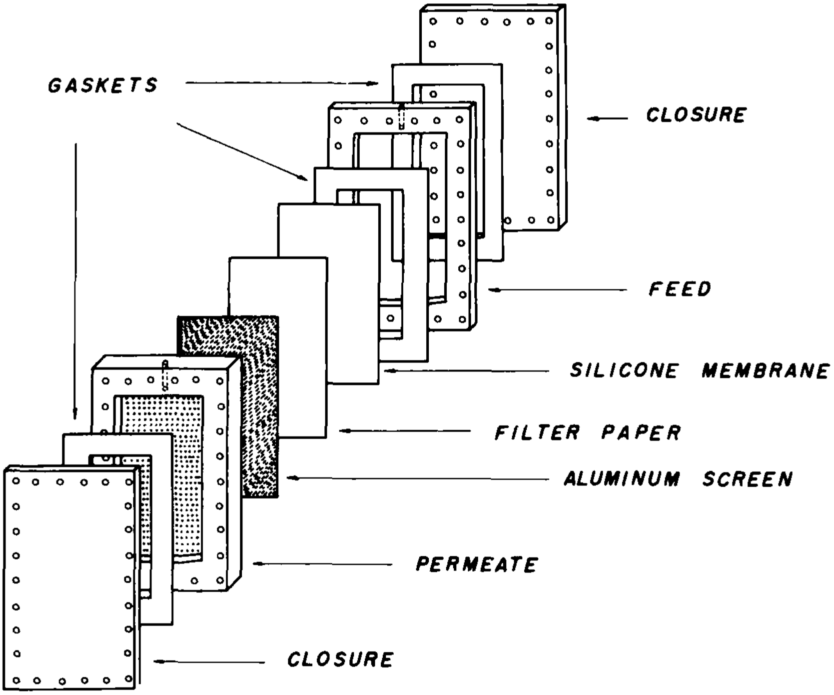

FIG. 1. Exploded view of the pervaporation cell.

The pervaporation experiments were performed according to the schematic description in Fig. 2. The cell and feed liquid reservoirs were filled and connected to a compressed N_2 cylinder, and the system was heated.

Permeate flow was determined by weighting the collected liquid. To determine its composition, the density was measured in an Anton Paar DMA 60-602 instrument.

Scanning electron micrographs were obtained in a Jeol T-300 microscope by using gold-coated samples. Membrane sections were prepared by freeze-fracture.

RESULTS

Ethanol and Acetone Pervaporation

Rates of ethanol and acetone pervaporation were determined as a function of temperature and pressure in membranes of various thicknesses.

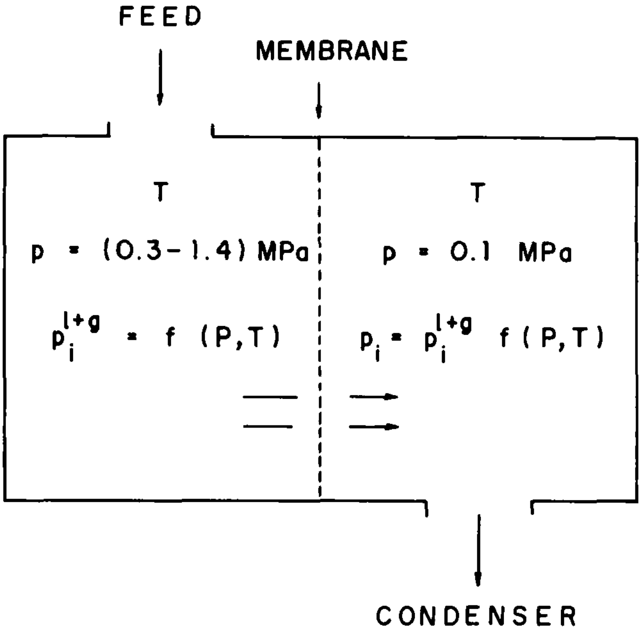

FIG. 2. Schematic description of pressure-driven pervaporation: p = pressure; p_i^{l+g} = vapor pressure of Component i; p_i = partial pressure of Component i.

The results are given in Figs. 3 to 7. The following observations can be made.

(a) At the lower temperatures, permeate flow increases with pressure; at the higher temperatures, it shows a small but negative pressure dependence. "Lower" temperatures mean temperatures below the ethanol boiling temperature at ambient pressure (76.7°C for ethanol and 54.3°C for acetone at 714 torr).
(b) The Arrhenius plots in Figs. 3 to 7 are nonlinear; steeper changes are observed at the normal ethanol boiling temperature.
(c) Large increases in permeate flow rates are observed with temperature at the lower feed pressures.

Together, these results show that high pervaporation outputs can be obtained by increasing the temperature at low but above-normal feed pressures, ca. 0.2 MPa.

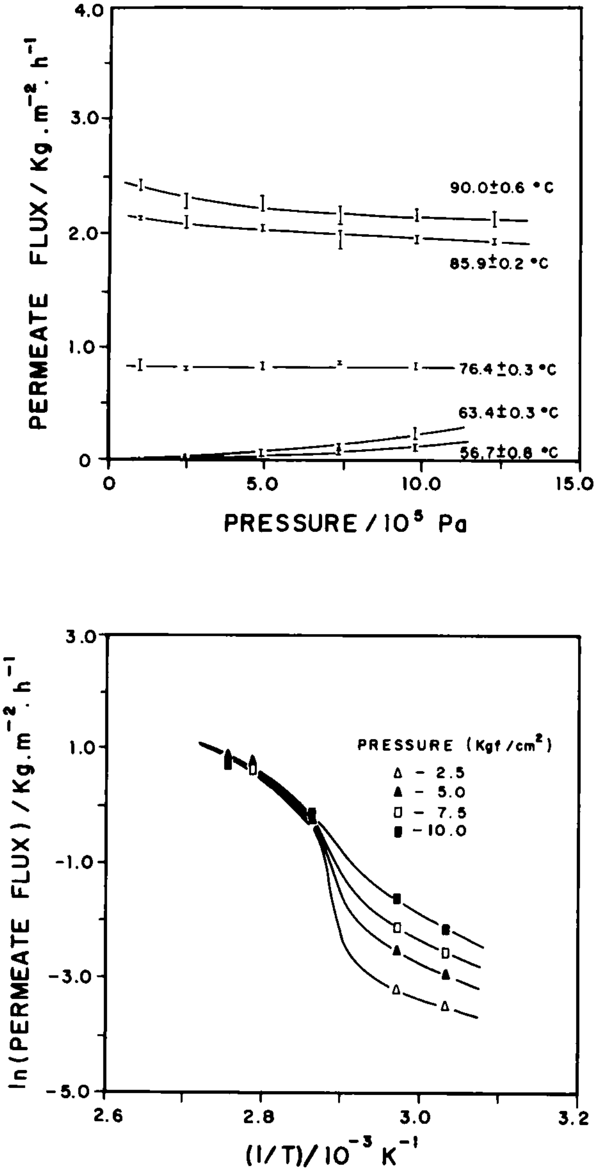

FIG. 3. Ethanol pervaporation through a 104-μm thick silicone dense membrane. Top: isotherms; bottom: isobars.

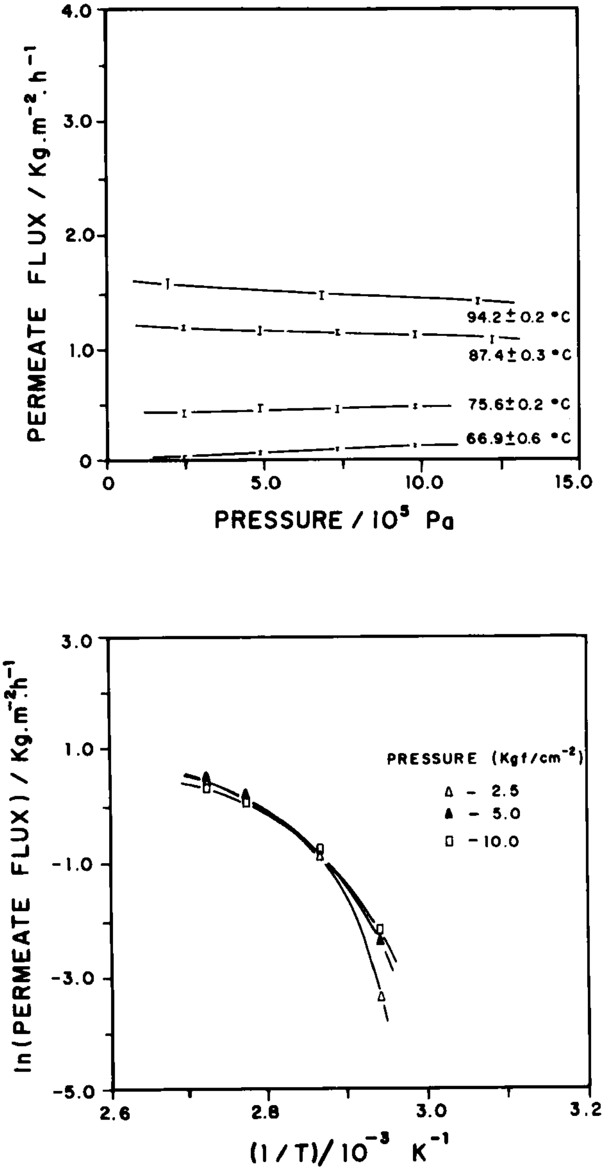

FIG. 4. Ethanol pervaporation through a 218-μm thick silicone dense membrane. Top: isotherms; bottom: isobars.

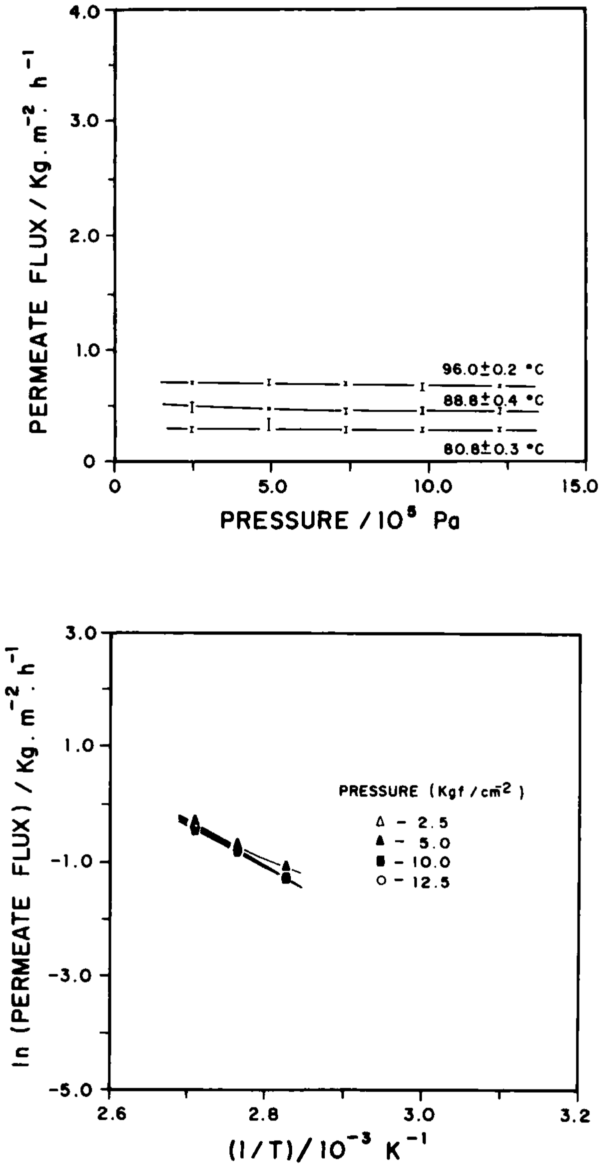

FIG. 5. Ethanol pervaporation through a 543-μm thick silicone dense membrane. Top: isotherms; bottom: isobars.

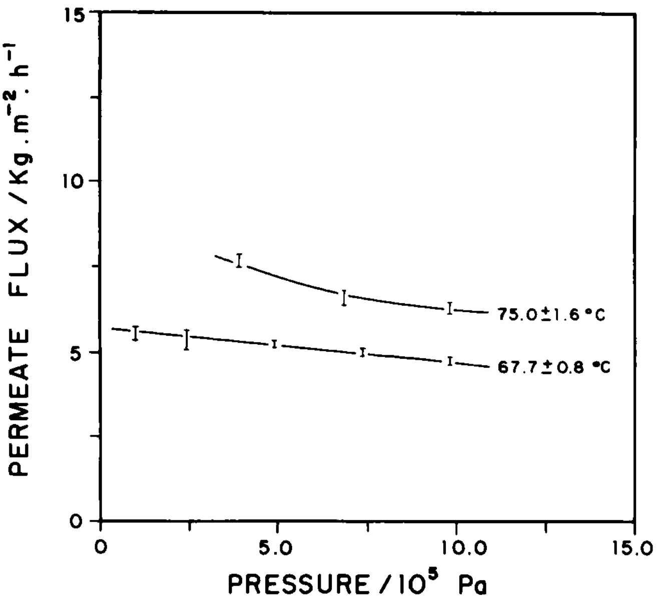

FIG. 6. Acetone pervaporation through a 101-μm thick silicone membrane.

Aqueous Ethanol Pervaporation

Aqueous ethanol pervaporation experiments were also performed under conditions analogous to these described in the previous section. Results of these experiments are in Table 1. High flow rates were obtained, even for ethanol feed concentrations below 10% (w/w).

Using these data, we plotted the ethanol concentrations in the permeate as a function of feed concentration. Data obtained at various feed concentrations, temperatures, and pressures cluster around a single line, as seen in Fig. 8. Moreover, we can observe in this figure that the concentration of the pervaporation permeate obtained from any feed concentration is higher than that of the vapor in equilibrium with this same feed liquid at normal pressure.

This means that one pervaporation step has a greater separation power than one theoretical plate in distillation for the set of concentration and other experimental conditions used here.

Membrane Morphology

Scanning electron micrographs were taken of the surfaces of the membranes as well as of the fracture surfaces obtained by bending films cooled

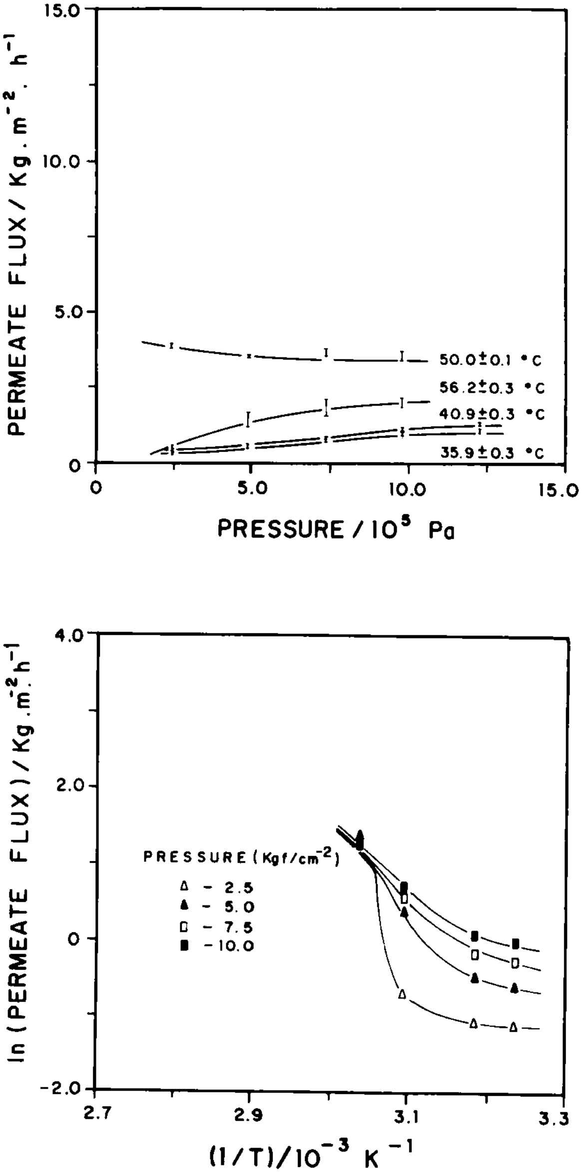

FIG. 7. Acetone pervaporation through a 86-μm thick silicone dense membrane. Top: isotherms; bottom: isobars.

TABLE 1
Pervaporation of Aqueous Ethanol Solutions

Temperature (°C)	Feed pressure (kgf/cm²)	Ethanol concentration (% w/w)		α, ethanol/water	Flux [g/(m²·h)]
		Feed	Permeate		
77.9	2.5	42.6	73.1	3.7	78
80.8	2.5	16.6	48.8	4.7	15
82.3	2.5	22.4	65.6	6.6	101
85.2	10.0	14.6	58.8	8.3	59
86.0	2.5	35.0	72.5	4.9	451
86.0	2.5	33.8	72.6	5.2	451
86.0	2.5	31.1	72.2	5.8	451
86.0	2.5	30.6	72.5	6.0	451
86.0	12.5	13.8	56.8	8.2	75
89.5	2.5	2.9	15.9	6.3	41
90.7	2.5	2.5	21.4	10.4	58
91.1	2.5	13.3	55.2	8.0	140
91.2	2.5	18.2	58.4	6.3	379
91.5	2.5	13.0	55.3	8.3	344
91.5	2.5	3.6	26.9	9.8	121
92.3	2.5	2.1	16.4	9.0	58
95.5	10.0	7.3	40.1	8.5	201
95.6	2.5	3.0	34.7	17.3	238
96.2	2.5	3.6	30.9	11.9	251
96.3	2.5	8.0	53.8	13.4	426
96.4	2.5	8.1	50.7	11.7	367
96.6	2.5	1.2	13.2	12.6	141
96.7	2.5	7.1	52.4	14.3	386
97.0	2.5	6.6	53.2	16.1	410
97.0	2.5	10.1	56.6	11.6	486
97.1	2.5	14.6	58.4	7.9	517
97.2	2.5	12.4	59.0	10.2	527

under liquid N_2. The micrographs (Fig. 9) show that the membranes do not have pores and voids at their surfaces.

DISCUSSION

The effect of temperature on pervaporation rates is rather pronounced, and it differs from what would have been predicted by assuming a constant activation energy for permeation (*6*).

Even though the separation factors determined for aqueous ethanol solutions do not have a clear temperature dependence, as was also found by other authors (*7*), it seems that the overall mechanism of pervaporation is

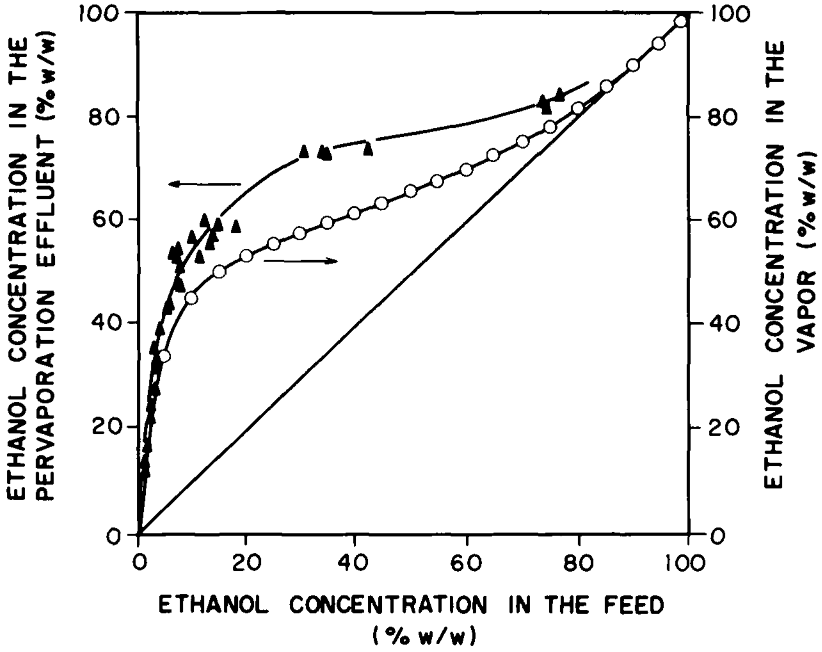

FIG. 8. Ethanol concentration in pervaporation effluent (▲) vs feed concentration. Ethanol concentration in vapor (○) in equilibrium with liquid.

temperature-dependent. Major features of flow vs pressure curves are completely different above and below the liquid boiling temperature.

Some assumptions can be made in an attempt to rationalize the results described in this paper.

(a) As opposed to what is assumed in the current pervaporation models, we assume that liquid desorption from the membrane contributes to limit the overall rate of pervaporation.

(b) We also consider that there is a strong decrease in the solubility of liquid in the membrane as the temperature rises above the boiling point of the liquid.

The first hypothesis has been discarded in the literature because the permeate is removed rapidly in conventional pervaporation (*8*), which points to diffusion through the membrane as the rate-limiting step. On the other hand, there is also experimental data in the literature (*6*, *9*) showing that the permeate flow rate increases when the pressure (on the permeate

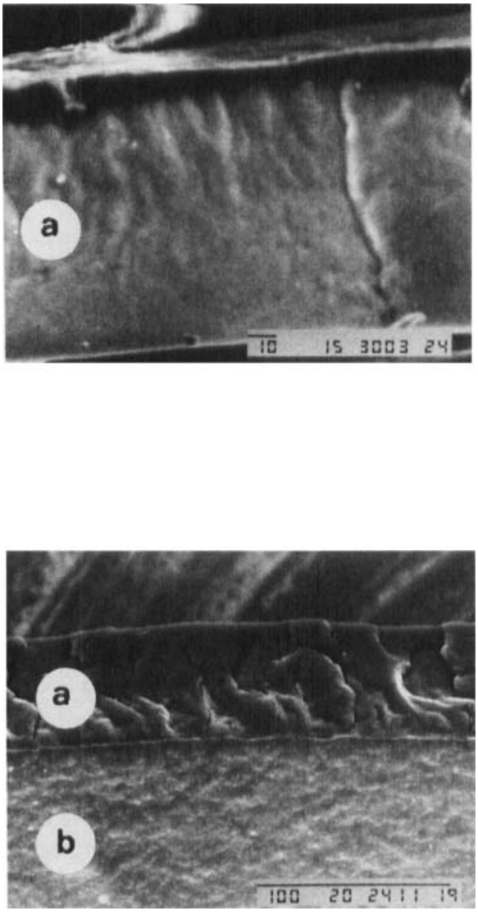

FIG. 9. SEM micrographs of dense PDMS membranes: (a) fracture surface; (b) cast surface.

side) drops. This shows that the desorption rate cannot be neglected in every case.

The second hypothesis is in agreement with the known general features of liquid–vapor diagrams of binary systems in which the boiling points differ widely. Taking the permeate–silicone as a binary liquid–liquid system, we expect its phase diagram should be depicted as in Fig. 10.

By using a higher pressure, a temperature above the normal boiling temperature on the feed side would mean that the membrane would be at a point like *F* in Fig. 10. However, the isothermal decrease in pressure throughout the membrane would bring the liquid to a two-phase region

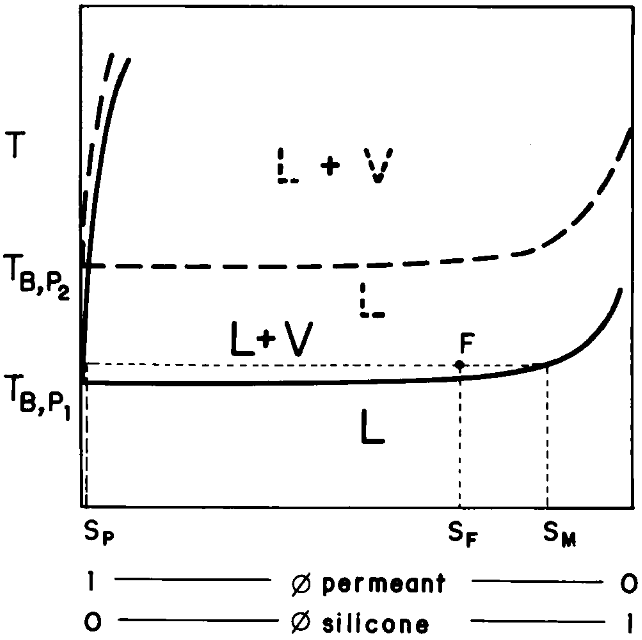

FIG. 10. Hypothetical phase diagrams for a binary system in which one of the components (the permeant) is much more volatile than the other (the membrane): (——) at room pressure; (- - -) at the feed pressure. S_F is the permeant concentration at $p > p_{\text{atm}}$ in the feed side; S_P is the permeant concentration in the effluent vapor phase at p_{atm}; S_M is the permeant concentration in the membrane in the effluent side.

on the permeate side. It is thus obvious that there would be a large decrease in permeant solubility or swelling coefficients across the membrane.

Swelling coefficients, as for any other partition coefficient, may be expressed as a ratio between sorption and desorption rates. A decrease in the swelling coefficient with temperature means that there is an increase in desorption rates relative to sorption rates.

We believe that the results presented in this work and the arguments raised above point to the need for more complete models for pervaporation. To take care of the present results, these models should consider not only solubility and diffusion but also the pressure dependence of solubility and desorption rates. Moreover, these models should include large membrane swelling coefficients.

Acknowledgments

This work was supported by grants from FAPESP and CNPq. D.W. is a PICD-CAPES predoctoral fellow.

REFERENCES

1. H. E. A. Brüschke, "Pervaporation Grossanlage Bétheniville," in *Aachener Membran Kolloquium,* 1989, Preprints, pp. 299–308.
2. J. W. Rhim and R. Y. M. Huang, *J. Membr. Sci., 46,* 335–348 (1989).
3. Z. Changluo, L. Moe, and X. Wei, *Desalination, 62,* 299–313 (1987).
4. M. C. Gonçalves, D. Windmöller, N. M. Erismann, and F. Galembeck, *Sep. Sci. Technol., 25,* 1079–1085 (1990).
5. D. Windmöller and F. Galembeck, "Poly(dimethylsiloxane) membranes in water-ethanol separation: behavior at higher temperatures," in *Polymers and Biomaterials* (H. Feng, Y. Han, and L. Huang, eds.), Elsevier, 1991, pp. 261–265.
6. C. S. Slater, P. J. Hickey, and F. P. Juricic, *Sep. Sci. Technol., 25,* 1063–1077 (1990).
7. J. M. Watson and P. A. Payne, *J. Membr. Sci., 49,* 171–205 (1990).
8. P. A. Néel and R. Clément, *Desalination, 53,* 297–326 (1985).
9. G. Bengtson and K. W. Böddeker, *Pervaporation of Low Volatiles from Water,* GKSS Forschungszentrum, Geesthacht, 1988.

Received by editor August 28, 1991